

Power Quality Improvement by Using Shunt Hybrid Power Filter and Thyristor Controlled Reactor with Fuzzy Logic Controller

Deepthi Venkat Cheerla, R. Madhusudhana Rao

Student, Power System Engineering(EEE), VR Siddhartha Engineering College, Andhra Pradesh, India.

Assistant Professor, Department of Electrical and Electronics Engineering, VR Siddhartha Engineering College, Andhra Pradesh, India.

Abstract—This paper proposes a combination of a three phase shunt hybrid power filter (SHPF) and a thyristor controlled reactor (TCR) for compensating harmonic currents and reactive power. The SHPF consists of a small rated voltage source inverter (VSI) in series with a 5th harmonic tuned LC passive filter. The rating of the VSI in the SHPF system is much smaller than that in the conventional shunt active power filter because the passive filter takes care of the major burden of compensation. The task of reactive power and harmonic compensation is shared by the combination of the SHPF and the TCR. The tuned passive filter and the TCR form a shunt passive filter (SPF) to compensate reactive power and consequently the SHPF is used to eliminate harmonic currents. The control of the SHPF is based on a nonlinear control technique method. The dynamic model of the SHPF system is first elaborated in the stationary 'abc' reference frame and then transformed into the synchronous orthogonal 'dq' reference frame. Fuzzy logic control is for the DC voltage and predictive control for the current. The DC voltage FLC handles the system uncertainties and nonlinearities, hence improving the transient performance. In addition, the proposed predictive current control technique features phase locked loop (PLL) independency. The simulation results are discussed, and the performance of the topology therefore evaluated.

Key Words: Shunt Hybrid Power Filter, Thyristor Controlled Reactor, Fuzzy Logic Controller and Harmonics.

1. INTRODUCTION

Power supply system suffers from serious problems of significant harmonics currents with poor input power factor caused by nonlinear loads. The line current harmonics cause increase in losses, instability, and also

voltage distortion. Traditionally, both passive and active filters have been used near harmonic producing loads or at the point of common coupling to block current harmonics. Shunt filters still dominate the harmonic compensation at medium/high voltage level, whereas active filters have been proclaimed for low/medium voltage ratings. Passive filtering has been preferred for harmonic compensation in distribution systems due to low cost, simplicity, reliability, and control less operation. Passive filters are found suitable with diverse applications involving reactive power together with harmonic compensation by thyristor switched filters (TSF) which contains many passive filters and the variation of load power can be adjusted [1]-[2]. The problems of passive filters can be mitigated by active filters have a good performance and more effective in harmonic compensation but for large scale system the active filter cost is high [3]-[11].

Hybrid filters soften effectively the problems of passive filter and an active filter solution and provide convenient harmonic compensation, particularly for high power linear loads [12] - [15]. Many techniques such as instant reactive power theory, synchronous rotating reference controller chassis, sliding mode, techniques of neural networks, nonlinear control, pre-control, Lyapunov function- based control [16]-[18], etc., have been used to improve the Performance Filters and hybrids.

Different topologies filter to compensate harmonics and reactive power has been reported in the literature [19] - [22]. In [19], an air conditioner consists of an active topology multi-converter by operating in parallel with a hybrid conditioner has conditioner It has been proposed. The hybrid air conditioner is constituted by one or more passive filters in series with a filter for rated active power low (APF). Conditioner compensates harmonic distortion, unbalance, and reactive power in three-phase four-wire systems. This topology provides a solution high-power level, which is convenient because of kilovolt ampere Rating Reduction inverters.

A hybrid basic configuration on the combination of a three-phase three-level neutral point blocked (NPC) inverter and a series connection of a level three H-bridge inverter with a control system to control the novel variable voltage generator stage H-bridge has been presented in [20]. In this topology, the inverters used to provide NPC the total active power, while the bridge is operating as series Filters for harmonic compensation output NPC Voltage. The rating of the active filter range is reduced because the latter only provides the reactive power for the operation of the floating capacitor. In [21], a combination of a thyristor controlled reactor (TCR) and a hybrid resonant impedance APF harmonic cancellation, load balancing, and reactive power compensation was

proposed. The control strategy the system is based on the voltage transformation vector to compensate for the reverse current caused by unbalanced load, without the use of phase locked loops. A predictive current controller based on Smith predictor is proposed to compensate for the waiting time generalized. A combined system a static var compensator (SVC) and a small-rated APF harmonic suppression and reactive power compensation has it was reported in [22]. The SVC is constituted by a Y connected power of passive filter and a delta-connected TCR. APF is used to eliminate harmonic currents and to avoid resonance between the filters and the impedance of the passive power.

2. SYSTEM CONFIGURATION OF SHPF-TCR COMPENSATOR

Fig. 1 shows the topology of the proposed combined SHPF and TCR. The SHPF consists of a small-rating APF connected in series with a fifth-tuned LC passive filter. The APF consists of a three-phase full-bridge voltage-source pulse width modulation (PWM) inverter with an input boost inductor (L_F, R_F) and a dc bus capacitor (C_{dc}). The APF sustains very low fundamental voltages and currents of the power grid, and thus, its rated capacity is greatly reduced. Because of these merits, the presented combined topology is very appropriate in compensating reactive power and eliminating harmonic currents in power system. The tuned passive filter in parallel with TCR forms a shunt passive filter (SPF). This latter is mainly for fifth harmonic compensation and PF correction. The small-rating APF is used to filter harmonics generated by the load and the TCR by enhancing the compensation characteristics of the SPF aside from eliminating the risk of resonance between the grid and the SPF. The TCR goal is to obtain a regulation of reactive power. The set of the load is a combination of a three phase diode rectifier and a three-phase star-connected resistive inductive linear load.

Fig.4.1 shows the topology of the proposed combined SHPF and TCR. The SHPF consists of a small-rating APF connected in series with a fifth-tuned LC passive filter. The APF consists of a three-phase full-bridge voltage-source pulse width modulation (PWM) inverter with an input boost inductor (L_F, R_F) and a dc bus capacitor (C_{dc}). The APF sustains very low fundamental voltages and currents of the power grid, and thus, its rated capacity is greatly reduced. Because of these merits, the presented combined topology is very appropriate in compensating reactive power and eliminating harmonic currents in power system. The tuned passive filter in parallel with TCR forms a shunt passive filter (SPF). This latter is mainly for fifth harmonic compensation and PF correction. The small-rating APF is used to filter harmonics generated by the load and the TCR by enhancing the compensation characteristics of the SPF aside from eliminating the risk of resonance between the grid and the SPF. The TCR goal is to obtain a regulation of reactive power. The set of the load is a combination of a three phase diode rectifier and a three-phase star-connected resistive inductive linear load.

MODELING OF SHPF AND TCR

2.1 SYSTEM CONFIGURATION OF SHPF-TCR COMPENSATOR

2.2 Modelling of SHPF

From fig 4.1 using Kirchhoff's voltage law,

$$v_{sa1} = L_F \frac{di_{ca1}}{dt} + R_F i_{ca1} + v_{CF1} + v_{O1} + v_{ON}$$

$$v_{sa2} = L_F \frac{di_{ca2}}{dt} + R_F i_{ca2} + v_{CF2} + v_{O2} + v_{ON}$$

$$v_{sa3} = L_F \frac{di_{ca3}}{dt} + R_F i_{ca3} + v_{CF3} + v_{O3} + v_{ON}$$

$$\frac{dv_{dc}}{dt} = \frac{1}{C_{dc}} i_{dc} \tag{1}$$

- The switching function c_i of the i^{th} leg of the converter (for $i=1,2,3$) is

$$c_i = \begin{cases} 1, & \text{if } S_i \text{ is On and } S'_i \text{ is Off} \\ 0, & \text{if } S_i \text{ is Off and } S'_i \text{ is On.} \end{cases} \quad (2)$$

• A switching state function d_{mi} is

$$d_{mi} = (c_i - \frac{1}{3} \sum_{n=1}^3 c_n) m \quad (3)$$

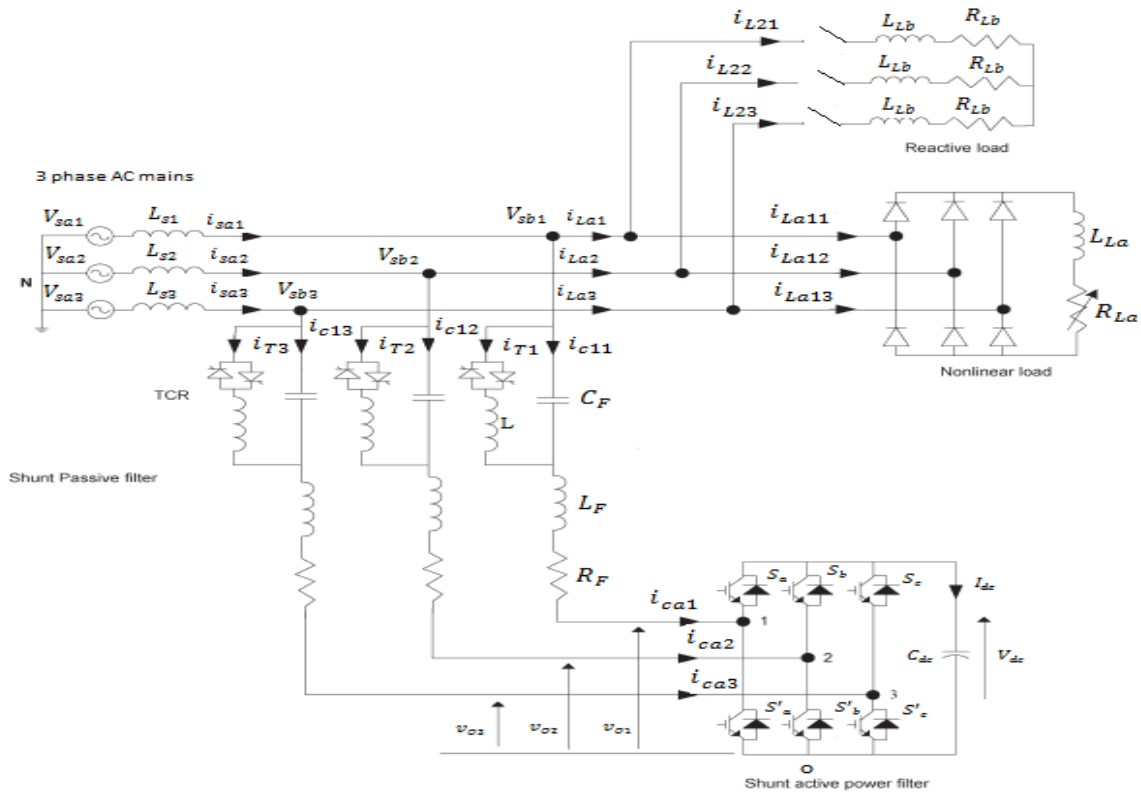


Fig. 1: Basic circuit of the proposed SHPF-TCR compensator

• The absence of the zero sequence in the AC currents and voltages and in the $[d_{nk}]$ functions leads to the following transformed model in the three phase coordinates.

$$L_F \frac{di_{ca1}}{dt} = -R_F i_{ca1} - d_{m1} v_{dc} - v_{CF1} + v_{sa1}$$

$$L_F \frac{di_{ca2}}{dt} = -R_F i_{ca2} - d_{m2} v_{dc} - v_{CF2} + v_{sa2}$$

$$L_F \frac{di_{ca3}}{dt} = -R_F i_{ca3} - d_{m3} v_{dc} - v_{CF3} + v_{sa3}$$

$$C_{dc} \frac{dv_{dc}}{dt} + \frac{v_{dc}}{R_{dc}} = d_{m1} i_{ca1} + d_{m2} i_{ca2} + d_{m3} i_{ca3} \quad (4)$$

Since the fundamental steady state components are sinusoidal, at the constant supply frequency synchronous orthogonal frame rotating the system is transformed.

$$C_{dq}^{123} = \frac{1}{\sqrt{3}} \begin{bmatrix} \cos \theta & \cos(\theta - 2\pi/3) & \cos(\theta - 4\pi/3) \\ -\sin \theta & -\sin(\theta - 2\pi/3) & -\sin(\theta - 4\pi/3) \end{bmatrix} \quad (5)$$

Where $\theta = \omega t$

- The existence of multiplication terms between the state variables $\{i_d, i_q, V_{dc}\}$ and the switching state function $\{d_{nd}, d_{nq}\}$ causes nonlinear and the model is time invariant during a switching state.
- Here the principle of operation of the SHPF requires that the three state variables have to be controlled independently.
- The interaction between the inner current loop and the outer DC bus voltage loop can be avoided by adequately separating their respective dynamics.

HARMONIC CURRENT CONTROL:

- A fast inner current loop and a slow outer DC voltage loop are adopted. The above two equations can be written as

$$\frac{dv_{dc}}{dt} = \frac{d_{md}}{C_{dc}} i_d + \frac{d_{mq}}{C_{dc}} i_q - \frac{v_{dc}}{C_{dc} R_{dc}}$$

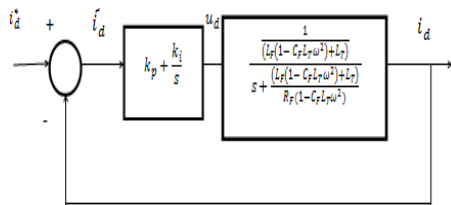


Fig 4.2: Inner control loop of the current.

- The currents i_d and i_q can be controlled independently. Moreover, by using proportional integral compensation, a fast dynamic response and zero steady state errors will achieve.
- The tracking controllers expressions are

$$u_d = (L_F(1 - C_F L_T \omega^2) + L_T) \frac{di_d}{dt} + R_F(1 - C_F L_T \omega^2) i_d$$

$$= k_p \tilde{i}_d + k_i \int \tilde{i}_d dt$$

$$u_q = (L_F(1 - C_F L_T \omega^2) + L_T) \frac{di_q}{dt} + R_F(1 - C_F L_T \omega^2) i_q$$

$$= k_p \tilde{i}_q + k_i \int \tilde{i}_q dt$$

(6)

- The transfer function of the above proportional integral controllers are

$$G_{i1}(s) = \frac{U_d(s)}{\tilde{i}_d(s)} = k_{p1} + \frac{k_{i1}}{s}$$

$$G_{i2}(s) = \frac{U_q(s)}{\tilde{i}_q(s)} = k_{p2} + \frac{k_{i2}}{s}$$

(7)

- The inner loop of the current i_d is as shown in the below figure
- The closed loop transfer functions of the current loops are

$$\frac{I_d(s)}{I_d^*(s)} = \frac{k_{p1}}{A} \frac{(s + \frac{k_{i1}}{k_{p1}})}{s^2 + (\frac{B + k_{p1}}{A})s + k_{i1}}$$

$$\frac{I_q(s)}{I_q^*(s)} = \frac{k_{p2}}{A} \frac{(s + \frac{k_{i2}}{k_{p2}})}{s^2 + (\frac{B + k_{p2}}{A})s + k_{i2}}$$

(8)

Where $A=L_F(1 - C_F L_T \omega^2) + L_T$ and $B=R_F(1 - C_F L_T \omega^2)$.

- The closed loop transfer functions of the current loops having the following form

$$\frac{I_d(s)}{I_d^*(s)} = 2\zeta\omega_{mi} \frac{(s + \frac{k_{i1}}{k_{p1}})}{s^2 + 2\zeta\omega_{mi}s + \omega_{mi}^2}$$

(9)

Where ω_{mi} =outer loop natural angular frequency

ζ =damping factor

DC BUS VOLTAGE REGULATION:

- In order to maintain the DC bus voltage level at a desired value, acting on i_q can compensate the losses through the hybrid power filter components.

$$C_{dc} \frac{dv_{dc}}{dt} + \frac{v_{dc}}{R_{dc}} = d_{mq} i_q$$

(10)

- The three phase filter currents are given by

$$\begin{bmatrix} i_{ca1} \\ i_{ca2} \\ i_{ca3} \end{bmatrix} = \sqrt{\frac{2}{3}} i_q \begin{bmatrix} -\sin\theta \\ -\sin(\theta - \frac{2\pi}{3}) \\ -\sin(\theta - \frac{4\pi}{3}) \end{bmatrix} \tag{11}$$

- The fundamental filter rms current I_{cr}

$$i_{cr} = \frac{i_q}{\sqrt{3}} \tag{12}$$

- The q axis active filter voltage v_{Oq} is expressed as

$$v_{Oq} = q_{mq} v_{dc} = -Z_{F1} i_{q1}^* \tag{13}$$

Where Z_{F1} the impedance of the passive is filter at 50Hz and i_{q1}^* is a DC component.

An equivalent input u_{dc} is

$$u_{dc} = q_{mq} i_q \tag{14}$$

The control effort of the DC voltage loop is

$$i_{q1}^* = \frac{v_{dc}}{-Z_{F1} i_q} u_{dc} \tag{15}$$

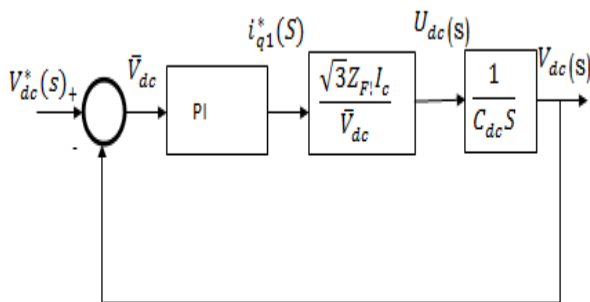


Fig 3: compensated voltage regulated model

To regulate the DC voltage V_{dc} , the error $\bar{V}_{dc} = V_{dc}^* - V_{dc}$ is passed the PI type controller is given by

$$u_{dc} = K_1 \bar{V}_{dc} + K_2 \int \bar{V}_{dc} \tag{16}$$

The response of the dc bus voltage loop is a second-order transfer function and has the following form:

$$\frac{V_{dc}(s)}{V_{dc}^*(s)} = 2\delta\omega_{nv} \frac{s + \frac{\omega_{nv}}{2\delta}}{s^2 + 2\delta\omega_{nv}s + \omega_{nv}^2} \tag{17}$$

The closed-loop transfer function of dc bus voltage regulation is given as follows:

$$\frac{V_{dc}(s)}{V_{dc}^*(s)} = \frac{\frac{\sqrt{3}Z_{F1}K_{PI}I_c}{\bar{V}_{dc}C_{dc}}s + \frac{\sqrt{3}Z_{F1}K_{PI}I_c}{\bar{V}_{dc}C_{dc}}}{s^2 + \frac{\sqrt{3}Z_{F1}K_{PI}I_c}{\bar{V}_{dc}C_{dc}}s + \frac{\sqrt{3}Z_{F1}K_{PI}I_c}{\bar{V}_{dc}C_{dc}}} \tag{18}$$

2.3 MODELING OF TCR:

- Using Kirchoff's voltage law, the following equations are obtained:

$$\begin{aligned} v_{sa1} &= L_T \frac{di_{LT1}}{dt} + L_F \frac{di_{ca1}}{dt} + R_F i_{ca1} + d_{m1} v_{dc} \\ v_{sa2} &= L_T \frac{di_{LT2}}{dt} + L_{PF} \frac{di_{ca2}}{dt} + R_F i_{ca2} + d_{m2} v_{dc} \\ v_{sa3} &= L_T \frac{di_{LT3}}{dt} + L_{PF} \frac{di_{ca3}}{dt} + R_F i_{ca3} + d_{m3} v_{dc} \end{aligned} \tag{19}$$

- Applying Park's transformation

$$\begin{aligned} L_T(\alpha) \frac{di_{LTd}}{dt} &= L_T(\alpha)\omega i_{LTq} + L_F\omega i_q - L_F \frac{di_d}{dt} - R_F i_d - d_{md} v_{dc} + v_d \\ L_T(\alpha) \frac{di_{LTq}}{dt} &= -L_T(\alpha)\omega i_{LTd} + L_F\omega i_d - L_F \frac{di_q}{dt} - R_F i_q - d_{mq} v_{dc} + v_q \end{aligned} \tag{20}$$

- The Reactive part is chosen to control the reactive current so that $v_q = 0$ and $L_f(\alpha)\omega_i L_T d = 0$

$$\frac{di_{Tq}}{dt} = B(\alpha)\omega[-L_F\omega i_d - L_F \frac{di_q}{dt} - R_F i_q - d_{mq} v_{dc}] \tag{21}$$

$B(\alpha) = 1/L_f(\alpha)\omega$ is the susceptance

- An equivalent input u_{qT} is

$$u_{qT} = \frac{di_{Tq}}{dt} \tag{22}$$

- Then

$$B(\alpha) = \frac{u_{qT}}{\omega[-L_F \omega i_d - L_F \frac{di_q}{dt} - R_F i_q - d_{nq} V_{dc}]} \quad (23)$$

$$\begin{aligned} \frac{di_q}{dt} + \frac{R_F(1-C_F L_T \omega^2)}{(L_F(1-C_F L \omega^2)+L_T)} i_q = \\ \frac{1}{(L_F(1-C_F L \omega^2)+L_T)} \left[+\omega(L_F(1-C_F L \omega^2)+L) i_d - \right. \\ \left. 2\omega C_F L \frac{d^2 v_{cfq}}{dt^2} + C_F L \frac{d^2 v_{cfq}}{dt^2} - (1-C_F L \omega^2) d_{nq} V_{dc} + \right. \\ \left. (1-C_F L \omega^2) V_q \right] \end{aligned} \quad (27)$$

The equivalent inductance is

$$L_F(\alpha) = L_F \frac{\pi}{2\pi+2\alpha+\sin(2\alpha)} \quad (24)$$

Then the susceptance is

$$B(\alpha) = B \frac{2\pi+2\alpha+\sin(2\alpha)}{\pi} \quad (25)$$

By replacing eq 27 in eq 6, we get

$$\begin{aligned} u_d = \frac{1}{(L_F(1-C_F L \omega^2)+L_T)} \left[\omega(L_F(1-C_F L \omega^2)+L) i_d - \right. \\ \left. (1-C_F L \omega^2) d_{nq} V_{dc} + (1-C_F L \omega^2) V_q \right] \\ u_q = \frac{1}{(L_F(1-C_F L \omega^2)+L_T)} \left[\omega(L_F(1-C_F L \omega^2)+L) i_d - \right. \\ \left. (1-C_F L \omega^2) d_{nq} V_{dc} + (1-C_F L \omega^2) V_q \right] \end{aligned} \quad (28)$$

Where $B=1/L_F(\alpha)\omega_0$

A PI controller is used to force the reactive current of the SHPF-TCR compensator to follow exactly the reactive current consumed by the load.

$$\frac{di_d}{dt} = \frac{1}{(L_F(1-C_F L \omega^2)+L_T)} \left[-R_F(1-C_F L_T \omega^2) i_d + \omega(L_F(1-C_F L \omega^2)+L) i_q - 2\omega C_F L \frac{d^2 v_{cfq}}{dt^2} + C_F L \frac{d^2 v_{cfq}}{dt^2} - (1-C_F L \omega^2) d_{nq} V_{dc} + (1-C_F L \omega^2) V_d \right]$$

From the above equation we get the control law they are represented as

$$\frac{di_q}{dt} = \frac{1}{(L_F(1-C_F L \omega^2)+L_T)} \left[-R_F(1-C_F L_T \omega^2) i_q + \omega(L_F(1-C_F L \omega^2)+L) i_d - 2\omega C_F L \frac{d^2 v_{cfq}}{dt^2} + C_F L \frac{d^2 v_{cfq}}{dt^2} - (1-C_F L \omega^2) d_{nq} V_{dc} + (1-C_F L \omega^2) V_q \right] \quad (29)$$

$$\frac{dV_{dc}}{dt} = \frac{d_{nd}}{C_{dc}} i_d + \frac{d_{nq}}{C_{dc}} i_q - \frac{V_{dc}}{R_{dc} C_{dc}} \quad (26)$$

$$\begin{aligned} d_{nd} = \frac{1}{(1-C_F L \omega^2) V_{dc}} \left[\omega(L_F(1-C_F L \omega^2)+L) i_q + \right. \\ \left. (1-C_F L \omega^2) V_q - (L_F(1-C_F L \omega^2)+L) u_d \right] \\ d_{nq} = \frac{1}{(1-C_F L \omega^2) V_{dc}} \left[\omega(L_F(1-C_F L \omega^2)+L) i_d + \right. \\ \left. (1-C_F L \omega^2) V_d - (L_F(1-C_F L \omega^2)+L) u_q \right] \end{aligned} \quad (30)$$

We can write the above equations as,

$$\begin{aligned} \frac{di_d}{dt} + \frac{R_F(1-C_F L_T \omega^2)}{(L_F(1-C_F L \omega^2)+L_T)} i_d \\ = \frac{1}{(L_F(1-C_F L \omega^2)+L_T)} \left[+\omega(L_F(1-C_F L \omega^2)+L) i_q - 2\omega C_F L \frac{d^2 v_{cfq}}{dt^2} + C_F L \frac{d^2 v_{cfq}}{dt^2} - \right. \\ \left. (1-C_F L \omega^2) d_{nq} V_{dc} + (1-C_F L \omega^2) V_d \right] \end{aligned}$$

3. RESULTS

3.1 SIMULINK MODEL OF PROPOSED SYSTEM WITHOUT COMPENSATION

The simulations were performed using the numerical simulator "Power System Block set" operating in Mat lab / Simulink, in order to verify the operation of the proposed compensator SHPF - TCR via nonlinear control.

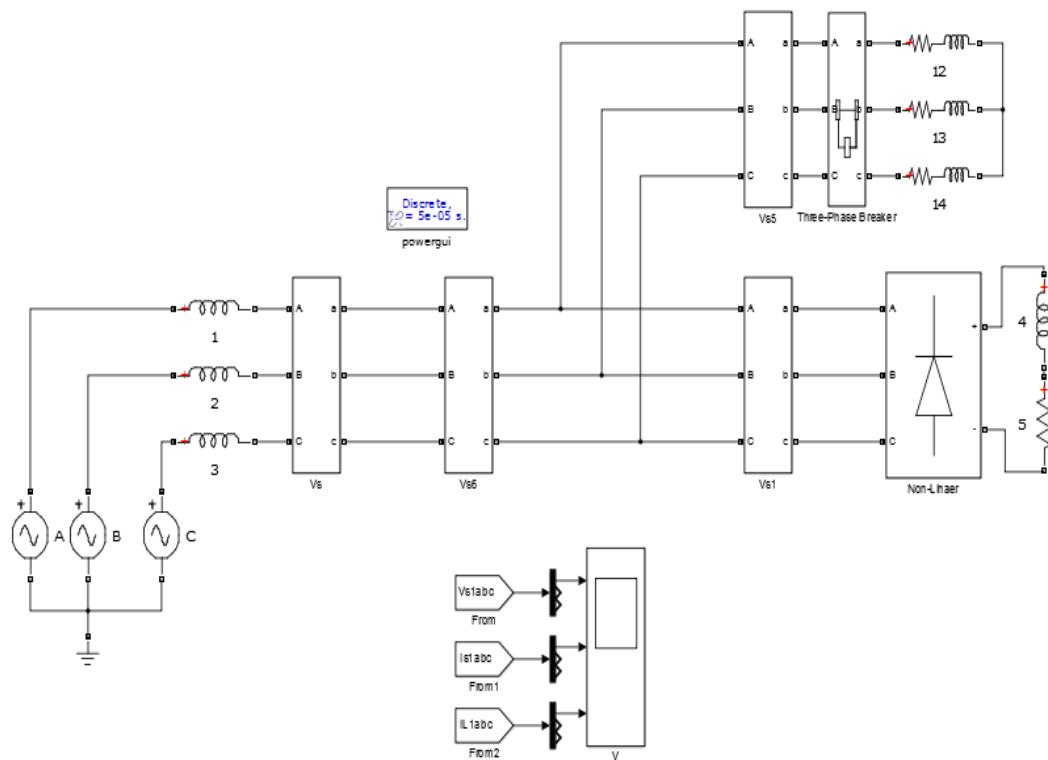


Fig 4: Proposed system with Linear And Non Linear Loads Simulation

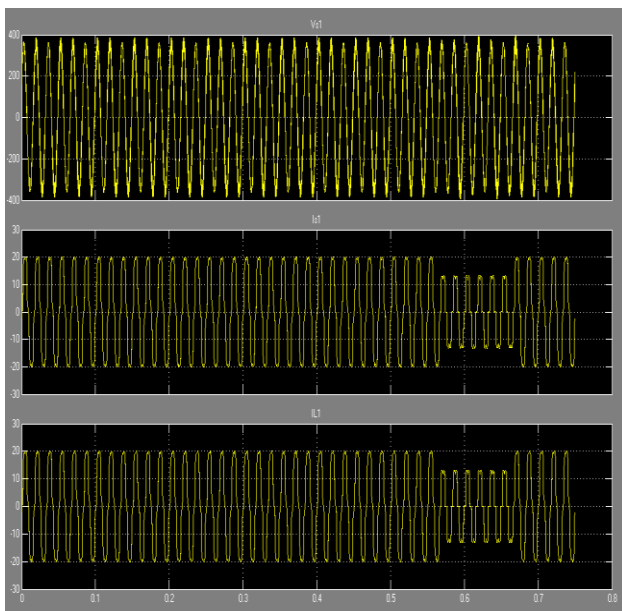


Fig 5: output waveforms for voltage at source, current at source and current at load.

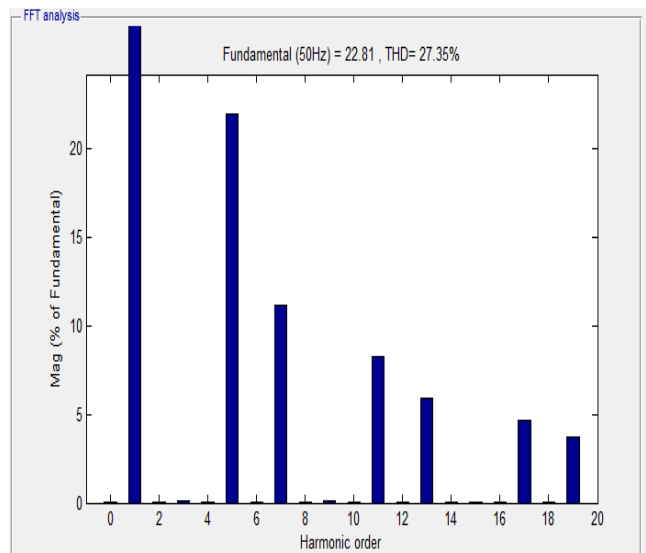


Fig 6: THD analysis for current at source without compensation

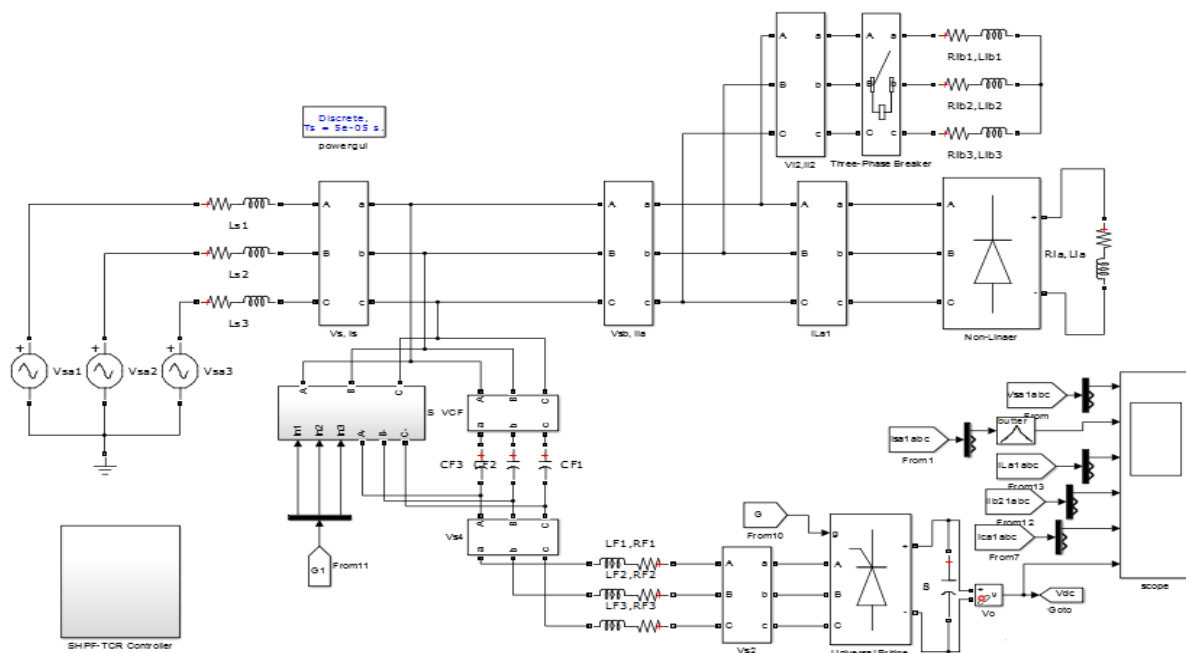


Fig. 7. simulink model of Shunt Hybrid Power Filter and Thyristor-Controlled compensation

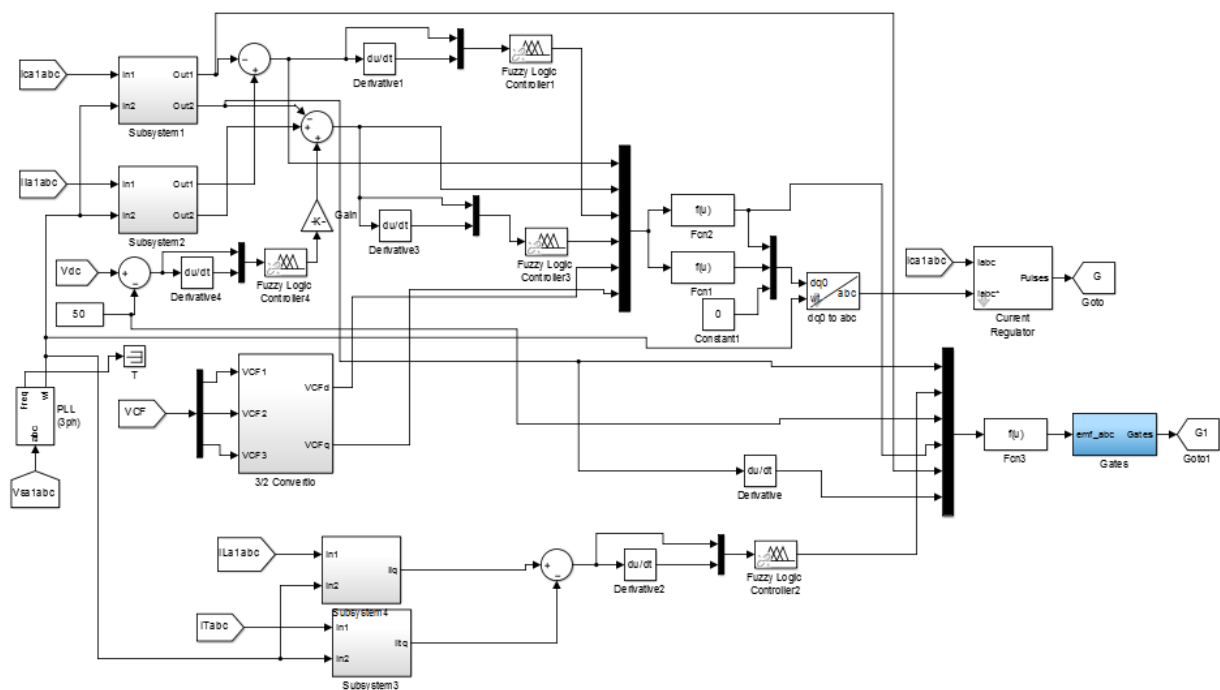


Fig. 8. control scheme SHPF-TCR compensator with fuzzy logic controller.

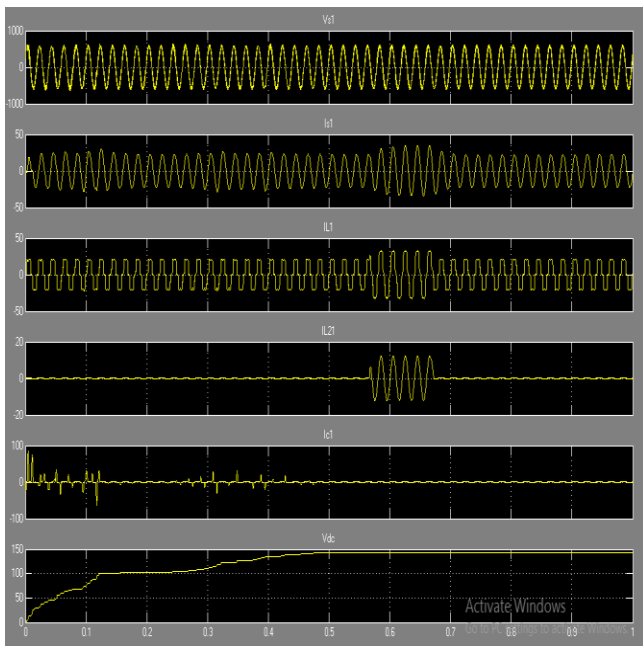


Fig.9.source voltage, source current, nonlinear load current, reactive load current, filters current , DC voltage for Shunt Hybrid Power Filter and Thyristor-Controlled with fuzzy.

TABLE: SPECIFICATION PARAMETERS

L-L source voltage and frequency	$V_s=440v; f_s=50Hz$
Line impedance	$L_s = 0.5mH; R_s = 0.1\Omega$
Nonlinear load	$L_{La} = 10mH; R_{La} = 27\Omega$
Linear load	$L_{Lb} = 20mH; R_{Lb} = 27\Omega$
Passive filter parameters	$L_f = 1.2mH, C_f = 240\mu F$
Active filter parameters	$C_{dc} = 3000\mu F, R_{dc} = 1K\Omega$
DC bus voltage of APF of SHAF	$V_{dc} = 50V$
Inner controller parameters	$K_{p1} = K_{p2} = 43.38$

	$K_{i1} = K_{i2} = 0.37408$
Outer controller parameters	$K_1 = 0.26; K_2 = 42$
TCR inductance	$L=25mH$

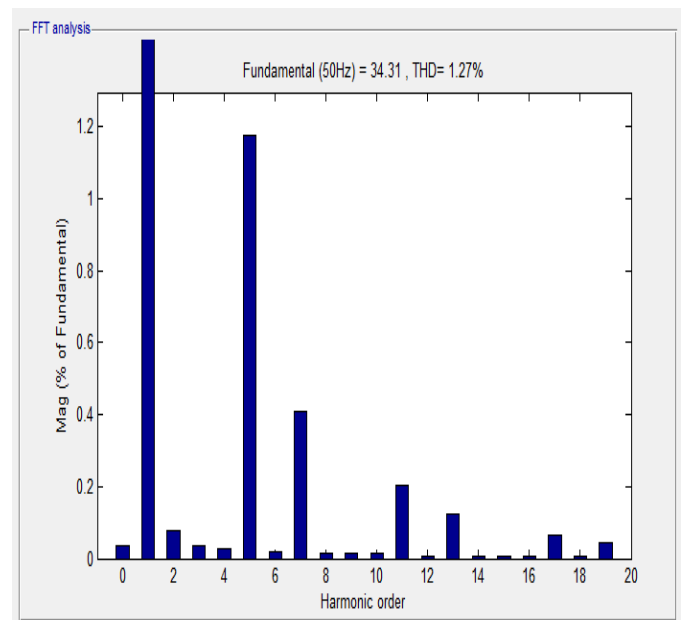


Fig. 10. Harmonic spectrum of source current in Shunt Hybrid Power Filter and Thyristor-Controlled with fuzzy.

CONCLUSION

In this project a SHPF-TCR compensator of a TCR and a SHPF has been proposed to achieve harmonic elimination and reactive power compensation. A proposed nonlinear control scheme of a SHPF-TCR compensator has been established, simulated, using Fuzzy controller. The shunt active filter and SPF have improved the performance of filtering and to reduce the power rating requirements of an active filter. It has been found that the SHPF-TCR compensator can effectively eliminate current harmonic and reactive power compensation of loads.

REFERENCES

- [1] Salem Rahmani, Abdelhamid Hamadi, "A Combination of Shunt Hybrid Power Filter and Thyristor-Controlled Reactor for Power Quality," *IEEE TRANSACTIONS ON INDUSTRIAL ELECTRONICS*, VOL. 61, NO. 5, MAY 2014.
- [2] A. Hamadi, S. Rahmani, and K. Al-Haddad, "A hybrid passive filter configuration for VAR control and harmonic compensation," *IEEE Trans. Ind. Electron.*, vol. 57, no. 7, pp. 2419–2434, Jul. 2010.
- [3] P. Flores, J. Dixon, M. Ortuzar, R. Carmi, P. Barriuso, and L. Moran, "Static Var compensator and active power filter with power injection capability, using 27-level inverters and photovoltaic cells," *IEEE Trans. Ind. Electron.*, vol. 56, no. 1, pp. 130–138, Jan. 2009.
- [4] H. Hu, W. Shi, Y. Lu, and Y. Xing, "Design considerations for DSP controlled 400 Hz shunt active power filter in an aircraft power system," *IEEE Trans. Ind. Electron.*, vol. 59, no. 9, pp. 3624–3634, Sep. 2012.
- [5] X. Du, L. Zhou, H. Lu, and H.-M. Tai, "DC link active power filter for three-phase diode rectifier," *IEEE Trans. Ind. Electron.*, vol. 59, no. 3, pp. 1430–1442, Mar. 2012.
- [6] M. Angulo, D. A. Ruiz-Caballero, J. Lago, M. L. Heldwein, and S. A. Mussa, "Active power filter control strategy with implicit closed loop current control and resonant controller," *IEEE Trans. Ind. Electron.*, vol. 60, no. 7, pp. 2721–2730, Jul. 2013.
- [7] X. Wang, F. Zhuo, J. Li, L. Wang, and S. Ni, "Modeling and control of dual-stage high-power multifunctional PV system in d-q-0 coordinate," *IEEE Trans. Ind. Electron.*, vol. 60, no. 4, pp. 1556–1570, Apr. 2013.
- [8] J. A. Munoz, J. R. Espinoza, C. R. Baier, L. A. Moran, E. E. Espinosa, P. E. Melin, and D. G. Sbarbaro, "Design of a discrete-time linear control strategy for a multicell UPQC," *IEEE Trans. Ind. Electron.*, vol. 59, no. 10, pp. 3797–3807, Oct. 2012.
- [9] L. Junyi, P. Zanchetta, M. Degano, and E. Lavopa, "Control design and implementation for high performance shunt active filters in aircraft power grids," *IEEE Trans. Ind. Electron.*, vol. 59, no. 9, pp. 3604–3613, Sep. 2012.
- [10] Y. Tang, P. C. Loh, P. Wang, F. H. Choo, F. Gao, and F. Blaabjerg, "Generalized design of high performance shunt active power filter with output LCL filter," *IEEE Trans. Ind. Electron.*, vol. 59, no. 3, pp. 1443–1452, Mar. 2012.
- [11] Z. Chen, Y. Luo, and M. Chen, "Control and performance of a cascaded shunt active power filter for aircraft electric power system," *IEEE Trans. Ind. Electron.*, vol. 59, no. 9, pp. 3614–3623, Sep. 2012.
- [12] S. Rahmani, A. Hamadi, K. Al-Haddad, and A. I. Alolah, "A DSP-based implementation of an instantaneous current control for a three-phase shunt hybrid power filter," *J. Math. Comput. Simul.—Model. Simul. Elect. Mach., Convert. Syst.*, vol. 91, pp. 229–248, May 2013.
- [13] C. S. Lam, W. H. Choi, M. C. Wong, and Y. D. Han, "Adaptive dc-link voltage-controlled hybrid active power filters for reactive power compensation," *IEEE Trans. Power Electron.*, vol. 27, no. 4, pp. 1758–1772, Apr. 2012.
- [14] A. Hamadi, S. Rahmani, and K. Al-Haddad, "Digital control of hybrid power filter adopting nonlinear control approach," *IEEE Trans. Ind. Informat.*, to be published.
- [15] A. Bhattacharya, C. Chakraborty, and S. Bhattacharya, "Parallel connected shunt hybrid active power filters operating at different switching frequencies for improved performance," *IEEE Trans. Ind. Electron.*, vol. 59, no. 11, pp. 4007–4019, Nov. 2012.
- [16] S. Rahmani, A. Hamadi, N. Mendalek, and K. Al-Haddad, "A new control technique for three-phase shunt hybrid power filter," *IEEE Trans. Ind. Electron.*, vol. 56, no. 8, pp. 2904–2915, Aug. 2009.
- [17] A. Luo, X. Xu, L. Fang, H. Fang, J. Wu, and C. Wu, "Feedback feedforward PI-type iterative learning control strategy for hybrid active power filter with injection circuit," *IEEE Trans. Ind. Electron.*, vol. 57, no. 11, pp. 3767–3779, Nov. 2010.
- [18] S. Rahmani, A. Hamadi, and K. Al-Haddad, "A Lyapunov-function-based control for a three-phase shunt hybrid active filter," *IEEE Trans. Ind. Electron.*, vol. 59, no. 3, pp. 1418–1429, Mar. 2012.
- [19] M. I. Milanés-Montero, E. Romero-Cadaval, and F. Barrero-González, "Hybrid multiconverter conditioner topology for high-power applications," *IEEE Trans. Ind. Electron.*, vol. 58, no. 6, pp. 2283–2292, Jun. 2011.
- [20] C. A. Silva, L. A. Cordova, P. Lezana, and L. Empringham, "Implementation and control of a hybrid multilevel converter with floating dc links for current waveform improvement," *IEEE Trans. Ind. Electron.*, vol. 58, no. 6, pp. 2304–2312, Jun. 2011.
- [21] A. Luo, S. Peng, C. Wu, J. Wu, and Z. Shuai, "Power electronic hybrid system for load balancing compensation and frequency-selective harmonic suppression," *IEEE Trans. Ind. Electron.*, vol. 59, no. 2, pp. 723–732, Feb. 2012.
- [22] A. Luo, Z. Shuai, W. Zhu, and Z. John Shen, "Combined system for harmonic suppression and reactive power compensation," *IEEE Trans. Ind. Electron.*, vol. 56, no. 2, pp. 418–428, Feb. 2009.

